

Overview of LHD (Large Helical Device) Project

FUJIWARA Masami*, MOTOJIMA Osamu, HAMADA Yasuji, WATARI Tetsuo, OKAMOTO Masao, SATOH Sadao, YAMAZAKI Kozo, SUDO Sigeru, NODA Nobuaki, OHYABU Nobuyoshi, YAMADA Hiroshi, KOMORI Akio, MITO Toshiyuki, KUBO Shin, TOI Kazuo, ICHIGUCHI Katsuji, KAWAHATA Kazuo, IMAGAWA Sinsaku, the LHD Group and IYOSHI Atsuo
The National Institute for Fusion Science, Toki 509-5292, Japan

(Received: 30 September 1997/Accepted: 22 October 1997)

Abstract

The Large Helical Device (LHD), the large scale superconducting helical device, is under construction at the National Institute for Fusion Science and is now in the last year of the 8-year construction schedule. The outline of the LHD program, the status of the on-site construction are described. The confinement and steady state operation are experimentally studied on high temperature plasmas relevant for fusion plasmas in a helical device with a size comparable with large tokamaks. The device will be completed at the end of 1997 and the initial operation, cooling down and the machine running will start from the beginning of 1998.

Keywords:

Large Helical Device, physics design, SC magnet technology, device construction and operation, experimental schedule

1. Introduction

LHD (Large Helical Device), the superconducting $\ell/m = 2/10$ helical device of R/a (the major/minor radius) = 3.9 m/0.6 m and $B = 3$ T, is constructed to develop a steady state fusion reactor [1]. The mission is accomplished by the realization of $\langle T_e \rangle = \langle T_i \rangle = 3-4$ keV, $\langle n \rangle = 10^{20} \text{ m}^{-3}$, and $\tau_E = 0.2-0.3$ s with 20 MW heating under $B = 4$ T. LHD has been designed based on the following guideline.

(1) The target plasma parameters are the several-10 keV temperature, $10^{13} \text{ cm}^{-3}-10^{14} \text{ cm}^{-3}$ density, and > 0.1 s energy confinement time, which cover non-dimensional parameters, the collisionality of ion and electron $\nu^* = qR/\lambda$ (the connection length divided by the mean free path) $10^{-3}-10^{-4}$ similar to that in fusion plasmas, $\langle \beta \rangle \sim 5\%$, etc.

(2) To realize these parameters based on the LHD scaling, which is now modified to ISS95 scaling, the device scale and the magnetic field were roughly deter-

mined $R \sim 4$ m, $B \sim 4$ T by the reasonable level of heating power 20-30 MW where the heating power density is similar to those of existing devices.

(3) The configuration has been selected as an $\ell = 2$ heliotron/torsatron configuration because of the existence of integrated data base and of the experience obtained from H-E/CHS/ATF construction.

(4) Other configuration parameters such as m , the toroidal mode number, γ , the pitch of the helical coils defined as ma_c/IR , a , the pitch modulation of the helical coils, and the required dipole/quadrupole fields are determined by MHD studies on β limit, particle confinement capability, the bootstrap current control etc.

(5) As another important factor to accomplish the LHD mission, steady state operation, the all coils are in the superconducting state and the continuous helical winding is employed to create the divertor structure with clean helical separatrixes for easy particle/heat

*Corresponding author's e-mail: fujiwara@nifs.ac.jp

control. Of course, the helical configuration is very sensitive to the coil structure and the real machine parameters are compromised with the SC technology requirements (Fig. 1 and Table 1).

These design procedures are quite different from the W7X design where the magnetic configuration is optimized for core plasma stability and confinement and then the coil structure is determined [2].

(6) The other important point is the flexibility of the configuration which is a powerful tool for study the optimum configuration for the plasma confinement. LHD coil system has various functions to satisfy these requirements. The change in γ by the independent operation of three blocks of helical winding can control $\iota(r)$, q_p , and shear. The three pairs of poloidal coils can control the position of the magnetic axis and the elongation of the plasma cross section. The $\ell/m = 2/10$

Table 1 The mechanical accuracy of LHD coils

<Errors of Fabrication of Helical Coils (3 σ)>				
	Bobbin (HC can)	Winding	Welding to Shell	Total
Minor radius	± 1.43	± 1.07	$< \pm 1.0$	$< \pm 2.1$ mm
Overtuning	± 1.50	$< \pm 0.75$	$< \pm 1.0$	$< \pm 2.0$ mm
Major radius (ave.)	-0.6	-0.3	-0.6	-1.5 mm

<Errors of Fabrication & Installation of Poloidal Coils>				
	Each Pancake	Coil (ave.)	Installation into Shell	Total
Major radius	$< \pm 2.0$	$< \pm 0.5$	$< \pm 1.0$	$< \pm 1.5$ mm
Height	-	$< \pm 0.5$	$< \pm 1.0$	$< \pm 1.5$ mm

helical coils consists of 2 independent coils which can be operated independently for the study of helical axis configurations.

2. Construction Status of LHD Device, Heating Devices and Diagnostics

LHD device construction had started from 1990 as the 8 years schedule and various R & D research for SC technologies, gyrotron development, NBI ion source, plasma facing components and others.

(1) Almost all of main components of LHD device were completed and are under installation into the cryostat. The key elements of LHD, helical coils (13 kA conductor using NbTi stabilized Al, pool boiling type cooling) and poloidal coils IV/IS/OV (21–31 kA NbTi conductor of cable in conduit type, forced flow cooling by SHe) have been already completed and installed in the cryostat fixed by the supporting shell structure. The mechanical accuracies, which are key parameters for obtaining clean nested magnetic surfaces, for helical coils and poloidal coils are listed in Table 2. The overall accuracies for helical coils are within 2 mm. Main components of the inaccuracy is considered to be $m = 10$ and lower mode number components are much lower. The thermal contraction (~ 10 mm) by the cooling down to 4.4 K is almost uniform in the major radial direction, and the expansion by the electromagnetic force under 3 T operation is 1.6 mm in the minor radial direction. These deformations do not contribute to low mode error fields, and the clean magnetic surface is obtained in LHD device.

The vacuum vessel (discharge chamber) is made by

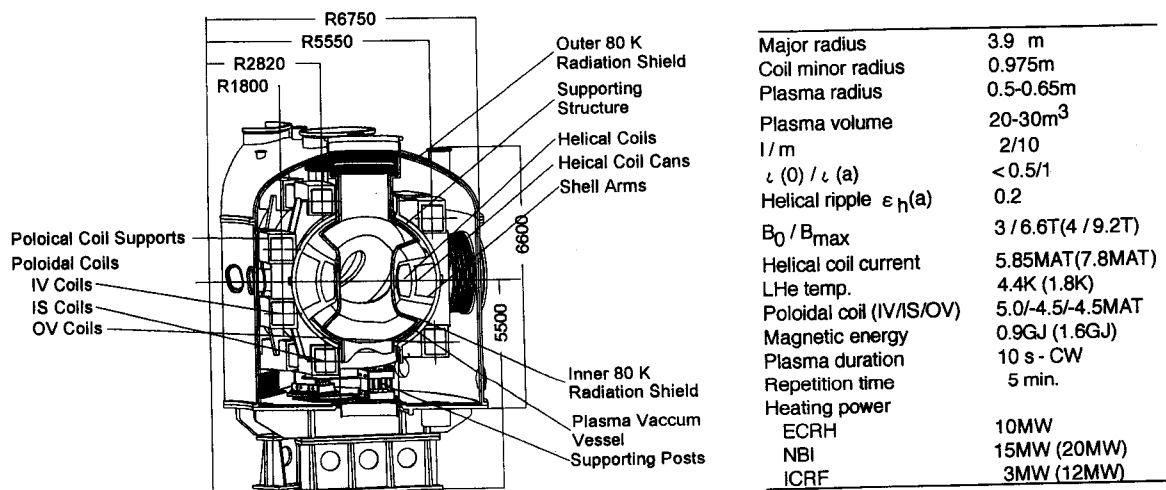


Fig. 1 The Cross-sectional view of LHD device and machine parameters

welding many stainless steel plates of which thickness is 15 mm. The vacuum vessel is covered with the first wall of 10 mm stainless plate which is cooled by water in order to operate plasmas in steady state heating.

(2) The coils, the supporting structure, and the discharge chamber are installed in the large cryostat. The coils and the supporting structure are fixed at the bottom plate of the cryostat through 10 cryogenic support columns. The discharge chamber is supported by the other structure and the port is connected to the outer cryostat port flange through the bellows to keep the discharge chamber free mechanically from the cryostat system.

(3) The helium refrigerator/liquefier has the cooling capability of 20.6 kW at 80 K, 5.67 kW at 4.4 K and 650 ℓ /hr. liquefaction. It also can deliver liquid helium of 650 ℓ /hr. simultaneously. These are enough for the requirement of 13.75 kW at 80 K, 2.05 kW at 4.4 K and 650 ℓ /hr in order to cool LHD coils, support structure, SC bus lines, 80 K shield and other components [3].

The superconducting bus lines are used to connect coils with power supplies which are placed 50–60 m away from the device in order to reduce large ohmic loss with conventional water cooled bus lines. The SC bus lines have been also installed [4].

(4) As the divertor experiments in LHD, the closed helical divertor fully around the torus is the final one to be studied. In the early experimental phase, however, LID (Local Island Divertor) and a local helical divertor are studied. The LID coil, which is used to control islands ($m/n = 1/1$ or $2/1$), is mounted on the cryostat. The LID coil can be also used to correct the low (m, n) error fields [5].

(5) The heating devices, ECH, NBI, and ICRF are prepared for LHD experiments. ECH is used for the plasma production and electron heating using two kinds of gyrotron 84 GHz and 168 GHz. The R&D results are 400 kW/10.5 s–500 kW/2 s for 84 GHz and 450 kW/0.1 s for 168 GHz. Two NBI injectors, which is

main heating method for ECH plasmas, are now under construction. The results using a test ion source are listed in Table 2 and the extracted negative ion beam current reaches 21 A, which is a half of the target value of 40 A/ion source, with 10 mrad. divergence and beam size. The ICRF heating system has been also developed and two kinds of launcher are prepared for the initial experiments using a half turn antenna for fast wave heating (1 MW level) and the folded wave guide for Ion Bernstein Wave heating (0.5 MW level).

(6) Various diagnostic instruments are also under construction, 12 channels FIR interferometer with 119 μm /CH₃OH Laser, YAG Thomson scattering system (200 channels/> 300 Hz repetition rate), and a normal incident VUV spectrometer. The bolometer systems is for local/global measurement of radiation with fast time and high spatial resolution. The Heavy Ion Beam Probe (6 MeV) is developed for the direct measurement of E_r . A multi-layer pellet is developed as the new diagnostic instrument.

3. Machine Build Up and Experimental Schedule of LHD

After the construction, the LHD is in operation by the following steps.

(1) Simultaneous pumping down of the cryostat and the discharge chamber by the use of pumping system which are TMP (5500 ℓ /s \times 2)/cryopump (25000 ℓ /s \times 2) for the cryostat (volume 900 m³, 10⁻⁵ Torr.) and TMP (5000 ℓ /s \times 2)/cryopump (43000 ℓ /s \times 2) for the discharge chamber (volume of 200 m³/surface area of 730 m², 3 \times 10⁻⁸ Torr).

(2) Cool-down procedure is as follows. First, 300 K to 80 K precooling will be accomplished by mixing of warm helium gas with LN₂ cooled helium gas. Further cool-down to \sim 6 K will be conducted with low temperature helium gas from the refrigerator. Finally, two-phase flow helium will be supplied to helical coils, supporting structures and SC bus-lines while poloidal coils utilize forced flow SH_e (0.97 MPa at 4.5 K) [6].

(3) The measurement of the magnetic surface using electron beam tracing is carried out by the use of the scanning fluorescent rod.

(4) As the first step of the discharge cleaning, 2.45 GHz/20 kW/CW ECH plasma is used to reduce the impurities such as oxygen sticking on the stainless steel first wall of the discharge chamber and T₁ gettering system is prepared as the back up. In the later stage, the boronization is possibly applied. The effective conditioning by LID (Local Island Divertor) is now under study.

Table 2 Test results of NBI

	No. of holes	I(H-) (A)	Beam Energy (keV)	Power (MW)	Duration (s)	Beam Diverge. (mrad.)	Beam Focus (cm)	
No.1	154 (13 ϕ)	5.5	104	0.57	0.6	10	24cm /10.4m	1/5 size
No.2	770 (13 ϕ)	21	106	2.22	0.6	10	24cm /10.4m	1/1 size
Target	770	40	180	7.2	10	10	52cm /13m	x2 sources /injctr.
2nd cycle	770	30x2	120	2.5	1-2	10	52cm /13m	x2 sources /injctr.

(5) The first cycle experiment is using two 84 GHz gyrotrons ($500 \text{ kW} \times 2/10 \text{ s}$) and possible use of 168 GHz gyrotrons ($400 \text{ kW} \times 2/2-3 \text{ s}$) for $B = 1.5 \text{ T}$ operation. The simple estimation under the following conditions is shown in Fig. 2.

$$n_e(r) = n_{e0}(1 - \rho^2)^{0.5} + 0.1 \text{ in the unit of } 10^{19} \text{ m}^{-3}$$

$$T_e(r) = T_{e0}(1 - \rho^2)^2 + 0.05 \text{ in the unit of keV}$$

$$T_i = 0.2 T_e, \text{ and } Z_{\text{eff}} = 1.6 \text{ (1\% Oxygen)}$$

Here, the impurity transport $D = 1 \text{ m}^2/\text{s}$ is assumed.

The fraction of the radiation loss determines the range of the operation plasma density and for 1MW ECH case as an example $2.5 \times 10^{19} \text{ m}^{-3}$ is expected to be a possible plasma density based on the experience of CHS experiments. The central electron temperature is 1.5 keV.

Diagnostics prepared for the 1st cycle experiment are 2 mm interferometer for n_i , ECE radiometer for $T_e(r)$, X-ray PHA for T_e and impurity contents, 12/20 channels bolometer using thin metal films for $P_{\text{rad}}(r)$, Visible spectrometer (200–700 nm) for $n_0(H)$ and T_i , and magnetic measurements such as magnetic probes, Rogowskii coils, and diamagnetic loops.

(6) The second cycle experiment is carried out in the later of 1998 by the use of ECH and NBI. The energy of NBI is 120 keV because of the lower field (1.5 T) operation and the power is 5 MW in total (2 injectors). The diagnostics available are FIR interferometer, Thomson scattering for $T_e(r)/n_e(r)$ and VUV spectrometer.

(7) At the end of FY1998, the machine is tested for 3 T operation and heating power is increased more. The

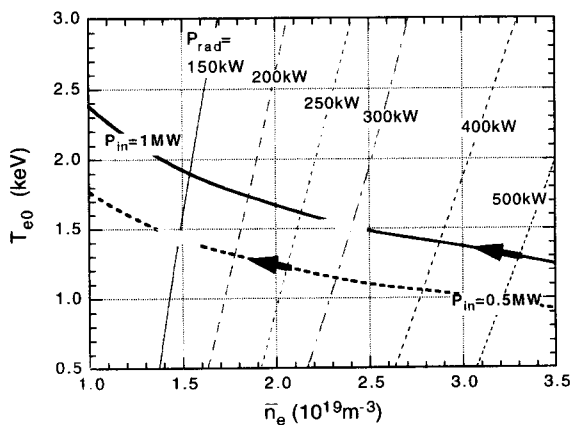


Fig. 2 The density and electron temperature estimated for ECH plasmas in the initial operation.

ECH is planned up to 3–9 MW using 168 GHz gyrotron and the power of NBI (180 keV) is raised up to 15 MW. ICRF power is also increased 3–9 MW.

(8) As for the divertor experiments, LID is tested in 1998–1999 and helical divertor is examined in the one pitch of helical structure [5].

(9) The steady state operation of 1 MW level is tried at first and gradually increased up to 3 MW depending on the development of the heat removal method in 1998–2000 [7].

The basic physics operation (the first phase of LHD project) is planned as described above [8]. The one of the most important issues to be studied is the confinement improvement to demonstrate the target parameters $\langle T_e \rangle = \langle T_i \rangle = 3 \text{ keV}$, $\langle n \rangle = 10^{20} \text{ m}^{-3}$, $\tau_E = 0.2 \text{ s}$ with 20 MW heating under $B = 3 \text{ T}$. The operation regimes in the physics phase are plotted in the $n\tau$ T-Top plane as shown in Fig. 3.

In the upgrade phase (2nd phase), the magnetic field is increased to 4 T by 1.8 K operation of the helical coil, the full helical divertor equipped with baffle plates, by which closed divertor operation is possible, will be installed and the D beam will be injected into D plasmas.

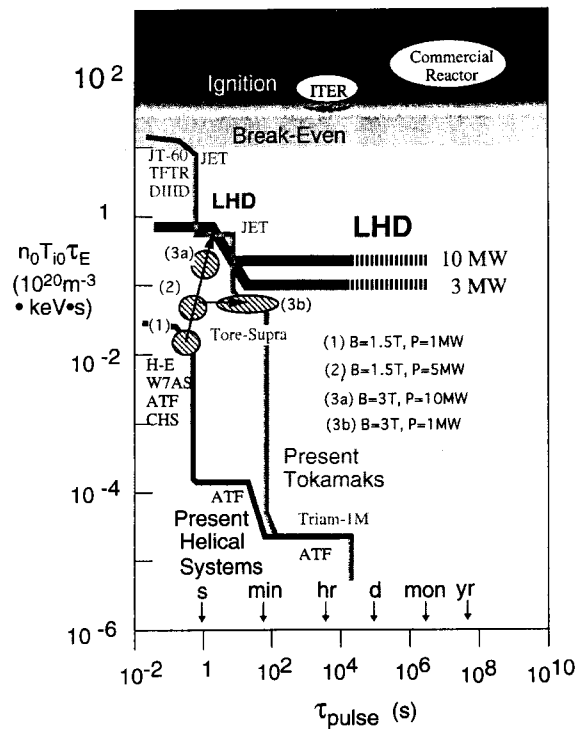


Fig. 3 The progress of LHD plasmas in $n\tau$ T-Top (the plasma duration).

References

- [1] A. Iiyoshi *et al.*, *Fusion Technology* **17**, 169 (1990); O. Motojima *et al.*, *13th International Conf. on Plasma Physics and Controlled Nuclear Fusion Research*, Washington, 1990, Vol.2, p.709 (1991); K. Yamazaki *et al.*, *13th International Conf. on Plasma Physics and Controlled Nuclear Fusion Research*, Washington, 1990, Vol.3, p.513 (1991); M. Fujiwara *et al.*, *The Proceeding of 10th International Conf. on Stellarators*, Madrid, Spain, p.175 (1995); M. Fujiwara *et al.*, *Plasma Phys. Control. Fusion* **39**, A261 (1997).
- [2] Wendelstein Group; *WENDELSTEIN VII-X, Application for Preferential Support*, IPP-EU-RATOM Association, 1990.
- [3] S. Satoh *et al.*, *Fusion Eng. Design* **20**, 129 (1993).
- [4] S. Yamada *et al.*, *IEEE Trans. on Magnetics* **32**, 2422 (1996).
- [5] A. Komori *et al.*, in these Proceedings, p.398 (1998); N. Ohya *et al.*, in these Proceedings, p.135 (1998).
- [6] T. Mito *et al.*, *Proc. CEC/ICMC* (1997), Portland, CPH3.
- [7] N. Noda *et al.*, in these Proceedings, p.130 (1998).
- [8] S. Sudo *et al.*, in these Proceedings, p.126 (1998).